[CANCER RESEARCH 58, 3765–3768, September 1, 1998]

Advances in Brief

Hypoxia and Vascular Endothelial Growth Factor Expression in Human Squamous Cell Carcinomas Using Pimonidazole as a Hypoxia Marker[1]

James A. Raleigh,[2] Dennise P. Calkins-Adams, Lillian H. Rinker, Cynthia A. Ballenger, Mark C. Weissler, Wesley C. Fowler, Jr., Debra B. Novotny, and Mahesh A. Varia

Departments of Radiation Oncology [J. A. R., D. P. C-A., L. H. R., C. A. B., M. A. V.], Surgery [M. C. W.], Obstetrics and Gynecology [W. C. F.], and Pathology [D. B. N.], University of North Carolina School of Medicine, Chapel Hill, North Carolina 27599

Abstract

Hypoxia in human tumors is associated with poor prognosis, but the molecular mechanisms underlying this association are poorly understood. One possibility is that hypoxia is linked to malignant progression through vascular endothelial growth factor (VEGF) induction and the associated angiogenesis and metastasis. The present clinical study measures hypoxia and VEGF expression on a cell-by-cell basis in human squamous cell carcinomas to test the hypothesis that hypoxia and VEGF protein expression are coupled in human tumors. Eighteen patients with invasive squamous cell carcinoma of the uterine cervix and head and neck have been investigated by a quantitative image analysis of immunostained sections from their tumors. The hypoxia marker pimonidazole was used to measure tumor hypoxia, and a commercially available antibody was used to measure VEGF protein expression. A quantitative immunohistochemical comparison of hypoxia and VEGF protein expression revealed no correlation between the two factors.

Introduction

VEGF[3]/vascular permeability factor is a family of M_r 34,000–42,000 homodimeric, disulfide-bonded glycoproteins that play a role in normal development and in tumor growth (1). VEGF is expressed as four isoforms: (*a*) VEGF 206; (*b*) VEGF 189; (*c*) VEGF 165; and (*d*) VEGF 121. The latter two isoforms are secretable. The promoter region of the *VEGF* gene has hypoxia-responsive elements that respond to hypoxia-inducible factor 1 (2, 3). Prolonged exposure to hypoxia can induce both VEGF mRNA and protein expression in mammalian cells (4, 5). Half-maximal induction of VEGF in isolated cells occurs in the range of 0.8–2.2% gas-phase oxygen concentration (5). On the basis of patterns of VEGF mRNA expression in human glioblastomas, Shweiki *et al.* (4) concluded that VEGF mRNA is also induced in hypoxic cells in solid tumors. These authors selected *in situ* analysis of VEGF mRNA over *in situ* immunodetection of the encoded protein because the localization of mRNA unequivocally identifies producer cells, whereas VEGF protein is secretable and can be sequestered at sites remote from the producing cells. However, it is the protein as measured by immunohistochemical analysis that correlates with microvascular density and poor prognosis in human tumors (6, 7); therefore, it is the protein that could link hypoxia to malignant progression (8, 9). An ideal complement to the immunohistochemical analysis of VEGF is the immunohistochemical analysis of hypoxia (10) based on the hypoxia marker pimonidazole (11–13). In the hypoxia marker approach, substituted 2-nitroimidazole compounds such as pimonidazole are activated and form protein adducts in mammalian cells at oxygen partial pressures less than 10 mm Hg (1.3% gas-phase concentration; Refs. 14 and 15). Adduct formation can be detected by specific antibodies and quantitated by means of image analysis (16). Pimonidazole hydrochloride was chosen as the hypoxia marker in the present study because of its high water solubility, chemical stability, low toxicity, and efficient tumor uptake. Excellent antibodies are available for the detection of pimonidazole adducts in formalin-fixed paraffin-embedded tissue sections in which the details of tissue architecture are well preserved (13). The prolonged lifetime of pimonidazole adducts in tumor tissue is an added benefit (12).

Materials and Methods

Pimonidazole hydrochloride (Hypoxyprobe-1) was obtained from Natural Pharmacia International, Inc. (Research Triangle Park, NC). Its structure, purity, sterility, and apyrogenicity were established by standard chemical and biological analyses. Reductive activation of pimonidazole hydrochloride in the presence of thiolated BSA by radiolytic means (17) provided a synthetic immunogen that was used by the North Carolina State University Hybridoma Facility (Raleigh, NC) to generate exhausted hybridoma supernatants for us by standard hybridoma techniques. After screening and isotyping in our laboratories, a supernatant containing an IgG1 monoclonal antibody (3.44.6.7) was selected for pimonidazole adduct detection. AEC, DAB, and Vectastain Elite ABC Kit (comprised of blocking serum, biotinylated antimouse IgG antibody, avidin, and biotinylated peroxidase; catalogue number PK-6102) were all obtained from Vector Laboratories (Burlingame, CA). Pronase, Brij 35, and Crystal/Mount were purchased from Biomeda Corp. (Foster City, CA). Aqua hematoxylin was obtained from Innovex Biosciences (Richmond, CA). An anti-VEGF rabbit polyclonal antibody preparation that recognizes the amino terminus of human VEGF 121, VEGF 165, and VEGF 189 isoforms was obtained from Santa Cruz Biotechnology, Inc. (Santa Cruz, CA). ProbeOn Plus glass slides and MicroProbe Staining Station were obtained from Fisher Scientific Co. (Norcross, GA).

Food and Drug Administration Investigational New Drug (IND) clearance was obtained for the use of pimonidazole hydrochloride as a hypoxia marker in human tumors (IND number 36,783). University of North Carolina at Chapel Hill Institutional Review Board approval was obtained for the clinical use of pimonidazole hydrochloride, and informed consent was obtained from all patients before entry into the study. The study was conducted in accordance with an assurance filed with and approved by the Office for Protection from Research Risk, Department of Health and Human Services. Protocol eligibility requirements were: (*a*) age greater than 18 years; (*b*) biopsy-confirmed carcinoma of the uterine cervix or head and neck; (*c*) informed consent according to an institutional review board-approved consent form; and (*d*) no concurrent sepsis or neuropathies. Laboratory requirements were: (*a*) hemoglobin > 8 g/dl; (*b*) serum creatinine < 2 mg/dl; and (*c*) serum bilirubin, aspartate aminotransferase, and serum alkaline phosphatase less than twice their normal values.

Pimonidazole hydrochloride at a whole-body dose of 0.5 g/m^2 at a concentration of 1.0 g/100 ml in normal saline was administered as an i.v. infusion lasting 20 min. Eighteen patients, 13 with uterine cervix tumors and 5 with

Received 5/13/98; accepted 7/16/98.

The costs of publication of this article were defrayed in part by the payment of page charges. This article must therefore be hereby marked *advertisement* in accordance with 18 U.S.C. Section 1734 solely to indicate this fact.

[1] Supported by Department of Health and Human Services National Cancer Institute Grants CA50995 and CA68826 and the State of North Carolina.

[2] To whom requests for reprints should be addressed, at Department of Radiation Oncology, University of North Carolina School of Medicine, CB# 7512, Chapel Hill, NC 27599. Phone: (919) 966-7710; Fax: (919) 966-7681; E-mail: raleigh@radonc.unc.edu.

[3] The abbreviations used are: VEGF, vascular endothelial growth factor; AEC, 3-amino-9-ethylcarbazole; DAB, 3,3′-diaminobenzidine; RT, room temperature.

head and neck tumors, were infused with pimonidazole hydrochloride in either the General Clinical Research Center or in an outpatient setting in the Department of Radiation Oncology at the University of North Carolina Hospitals. At 16–24 h after pimonidazole hydrochloride infusion, multiple punch biopsies were obtained from geographically distinct areas of the tumors. The stability of pimonidazole adducts *in vivo* (12) permits considerable latitude in the interval between pimonidazole hydrochloride infusion and tumor biopsy. Biopsies were obtained from all quadrants of the tumor whenever possible, whereas regions of obvious necrosis were avoided.

Fresh tumor biopsy samples were placed immediately in cold 10% neutral buffered formalin, kept on ice for 12–24 h, and then processed into paraffin blocks. Before immunostaining, three contiguous 4-μm sections from each paraffin-embedded biopsy sample were placed on ProbeOn Plus slides. One tissue section per biopsy was stained with H&E to confirm the presence of the tumor. The remaining two sections were immunostained for pimonidazole binding and VEGF, respectively.

In the case of immunostaining for pimonidazole adducts, tissue sections were deparaffinized with xylene and rehydrated with a graded series of aqueous ethanol solutions and deionized water, followed by a rinse with 10 mM PBS containing 0.2% v/v Brij 35 (PBS-Brij 35) at RT. The rehydrated sections were incubated for 20 min at 40°C with 3% v/v hydrogen peroxide in PBS-Brij 35 to quench endogenous peroxidase and then rinsed with PBS-Brij 35. These steps were carried out with the slides held vertically. Subsequent incubation steps were performed at RT (40°C for the Pronase step) under humidity control with the slides held horizontally. The sections were washed between each step with PBS-Brij 35. The sections were incubated for 25 min with Pronase in the case of cervical tumors or for 40 min in the case of head and neck tumors to unmask antigens. The sections were incubated for 30 min with blocking serum, for 1 h with a 1:100 dilution of the antipimonidazole IgG1 (3.44.6.7) supernatant in PBS containing 1% blocking serum, for 30 min with biotinylated antimouse IgG antibody (Vectastain Elite ABC Kit), and finally, for 30 min with streptavidin and biotinylated peroxidase-conjugated antibody complex (Vectastain Elite ABC Kit). The sections were treated with AEC for 20 min at RT and then for 45 s with aqua hematoxylin at RT. The slides were washed with deionized water and heated at 80°C for 20 min with Crystal/Mount.

For VEGF detection, tissue sections were immunostained in a manner similar to that used for pimonidazole adducts, except that the Pronase digestion step was omitted, and the sections were treated with the peroxidase chromogen DAB for 5 min at RT. The intensity of immunostaining for VEGF varied among areas in the tissue sections, and the data were recorded in subcategories of heavy, light, and total immunostaining.

Positive and negative immunostaining controls for pimonidazole adducts and VEGF consisted of tissue sections from a squamous cell carcinoma of the cervix that were known to contain both pimonidazole adducts and VEGF. In the case of positive controls, staining patterns and intensities for pimonidazole adducts and VEGF were constant from staining session to staining session. In the case of negative controls, primary antibodies for pimonidazole adducts and VEGF were omitted from the staining procedure. The negative controls were consistently free of nonspecific background staining. The Vectastain Elite ABC Kit used in the present investigation produced staining patterns and intensities that were indistinguishable from an earlier immunostaining procedure (13) but had the advantage of taking less time.

For image analysis of the immunostained tissue sections, the color detection threshold and default width settings were chosen for each peroxidase chromogen (AEC red for pimonidazole binding and DAB brown for VEGF) on the basis of an intensely immunostained region at ×200 magnification. The settings for each chromogen were optimized for intensity, saturation, and hue. Cells immunostained for pimonidazole binding above the threshold intensity were scored as labeled, with no distinction being made between light and heavy labeling. It is assumed that all cells labeled with pimonidazole adducts were at oxygen partial pressure <10 mm Hg in the tumor tissue (15). Multiple fields (4–21 fields, depending on the section size) from one section from each biopsy were captured at ×200 magnification by means of an Axioskop 50 microscope and a Fluar ×20 objective (Carl Zeiss Inc., Thornwood, NY) linked through a high-resolution three-chip video camera (Carl Zeiss Inc.; model ZVS-3C750E) to a high-resolution Sony Trinitron color monitor (model PVM 1343 MD) and a 486/33 microprocessor workstation running Image-1 software (Universal Imaging Corp., West Chester, NY). The mean percentage area immunostained in each field was calculated as a percentage of the total field area minus acellular space, stroma, necrosis, and host cells. This was repeated for each of the fields in each section from each biopsy. There were three to six biopsies/tumor available for most analyses, except for tumors 3, 6, 9, and 14, for which only two, one, two, or two biopsies, respectively, were available (Table 1).

Table 1 *Stage and number of biopsies analyzed for the squamous cell carcinomas investigated*

Tumor no.	Type	Stage	No. of biopsies analyzed
1	Cervix	Ib	4
2	Cervix	IIIb	6
3	Cervix	IIIb	2
4	Cervix	IIb	5
5	Cervix	IIIb	4
6	Cervix	Ib	1
7	Head and neck	$T_4N_3M_0$	5
8	Cervix	IIb	4
9	Head and neck	$T_3N_{2b}M_0$	2
10	Cervix	IIb	4
11	Head and neck	T_2N_1	4
12	Cervix	IIb	3
13	Cervix	IIIb	4
14	Head and neck	$T_4N_0M_0$	2
15	Cervix	IIIb	3
16	Cervix	IIIb	3
17	Head and neck	$T_3N_{2b}M_0$	3
18	Cervix	IIIb	4

In addition to measuring VEGF and pimonidazole binding on a tumor-by-tumor basis, tissue sections from the most hypoxic tumors were subjected to further microregional examination. Microscopic fields (×200) that contained both pimonidazole adducts and VEGF were selected from among all tissue sections, irrespective of the biopsies from which the sections were derived. A further selection was made on the basis that >1% of the field area must be immunostained for pimonidazole adducts. Typically, tissue sections from the most hypoxic tumors contained four to eight such fields. VEGF was then quantitated in each field. The objective was to discover if a correlation between hypoxia and VEGF expression might exist at the microregional level, even when a correlation between hypoxia and VEGF was absent at the overall tumor level.

Results

Cells immunostained for pimonidazole adducts were adjacent to regions of necrosis, but there was no staining within the necrotic regions, and the cells that were immunostained seemed to be healthy (*i.e.*, not pyknotic; Fig. 1*A*). In some instances, VEGF appeared to colocalize with cells immunostained for pimonidazole adducts (Fig. 1*B*), but this was not the predominant pattern. Cells immunostaining for VEGF tended to be farther removed from necrosis than did cells that contained pimonidazole adducts (Fig. 1*B*).

Fig. 1, *A* and *B*, is representative of only one pattern of VEGF expression in which both pimonidazole adducts and VEGF appeared in the same field of view. Other patterns included ones in which tumor microregions possessed pimonidazole adducts but lacked VEGF protein expression and in which microregions expressed VEGF but lacked pimonidazole adducts (photomicrographs not shown).

On a tumor-by-tumor basis, the highest levels of VEGF protein expression were associated with the most hypoxic tumors, but not all of the most hypoxic tumors had high levels of VEGF expression. Furthermore, many of the least hypoxic tumors had substantial levels of VEGF protein expression (Fig. 2). Overall, there was no correlation between the two factors. The data presented in Fig. 2 compare total VEGF immunostaining (heavy immunostaining plus light immunostaining) with pimonidazole binding on contiguous sections from each biopsy. A similar lack of correlation was observed when heavy VEGF immunostaining alone was compared with pimonidazole binding (data not shown).

At the microregional level, VEGF expression and pimonidazole

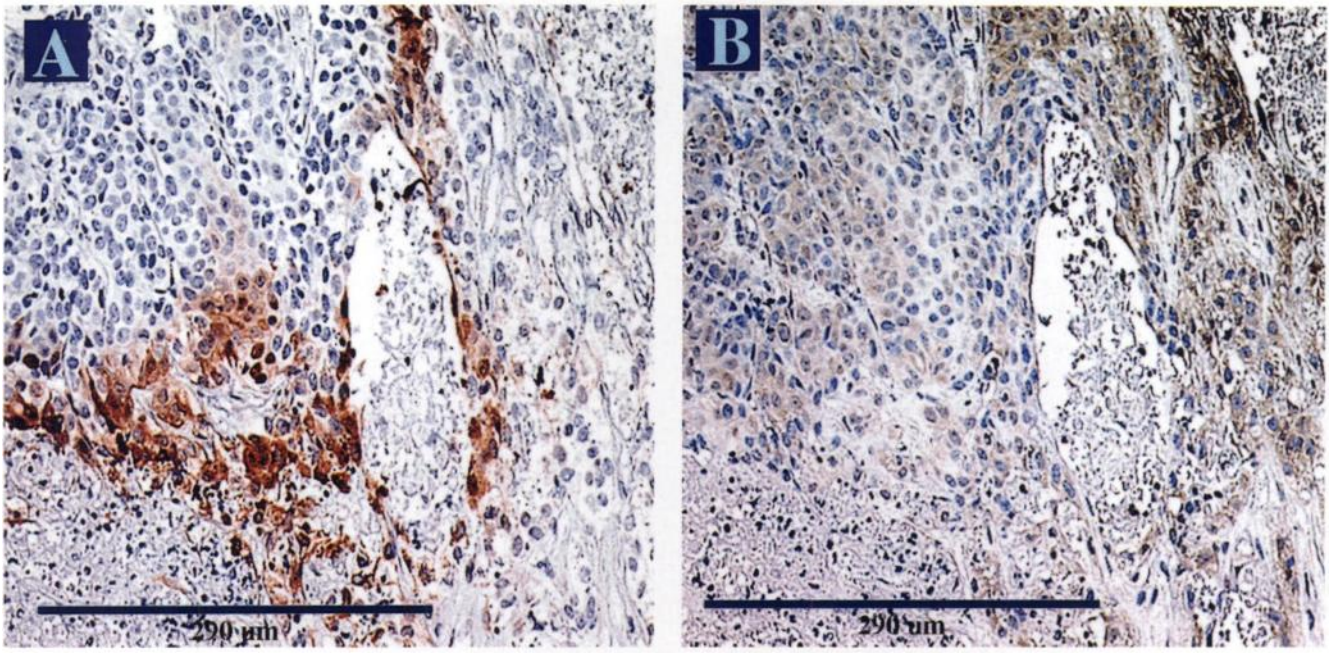

Fig. 1. Photomicrographs of the immunostaining for pimonidazole binding (*A*) and VEGF protein expression (*B*) in contiguous 4-μm sections from a formalin-fixed paraffin-embedded biopsy sample from a squamous cell carcinoma of the uterine cervix (×200). In *B*, the *upper right quadrant* contains an example of heavy VEGF immunostaining, and the *upper left quadrant* contains an example of light VEGF immunostaining. VEGF expression seems to be present in cells that are labeled with pimonidazole adducts, but much of the VEGF protein expression occurs in cells adjacent to those labeled with pimonidazole. This figure shows an example of a microscopic field in which immunostaining for both pimonidazole adducts and VEGF occurs. However, VEGF was often detected in the absence of pimonidazole staining and *vice versa*. *Bar*, 290 μm.

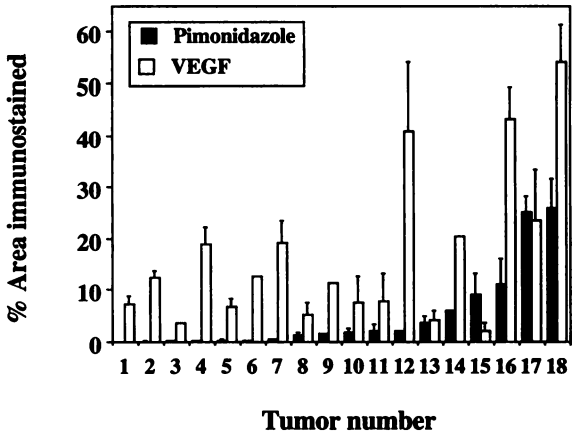

Fig. 2. Comparison between pimonidazole binding and VEGF expression in squamous cell carcinomas of the cervix and head and neck, arranged in order of increasing hypoxia from *left* to *right*. The data are the means ± SE of a quantitative image analysis of three or more biopsies taken from each patient, with the exception of tumors 3, 6, 9, and 14, for which one or two biopsies were available. Although the highest levels of total VEGF (heavy immunostaining plus light immunostaining) are associated with the most hypoxic tumors, no overall correlation between hypoxia and VEGF protein expression was seen.

binding were not correlated in microscopic fields that possessed high levels of pimonidazole binding (>1% of the area labeled). This was true for total VEGF immunostaining (Fig. 3) or for heavy VEGF immunostaining alone (data not shown).

There was no correlation between hypoxia or VEGF and tumor stage in the group of tumors studied.

Discussion

The present study is the first attempt to measure hypoxia and VEGF protein expression on a cell-by-cell basis in human tumors. Although VEGF is hypoxia inducible and can be correlated with microvessel density and tumor prognosis (6, 7), the present study indicates that the linkage between tumor hypoxia and prognosis is not simply through hypoxia-induced VEGF measured at the time of clinical presentation. This is true whether the comparison is made on a tumor-by-tumor basis (Fig. 2), or whether the comparison is made with a subset of data derived from microregions within the most hypoxic biopsy specimens, where the putative link between hypoxia and VEGF protein expression might be strongest (Fig. 3). It might be thought that hypoxic tumor cells exist in regions of low vascularity, and therefore a correlation between hypoxia and VEGF would not be expected, because the target for VEGF action, blood vessel endothelial cells, is not in close proximity to the hypoxic cells. However, the hypoxia marker approach shows that hypoxic cells are found within 10–12 cell diameters of blood vessels; therefore, on a microregional basis, hypoxic tumor cells are, in fact, reasonably close to the target of VEGF action.

There are a number of possible reasons for the lack of correlation between hypoxia as measured by the hypoxia marker approach and

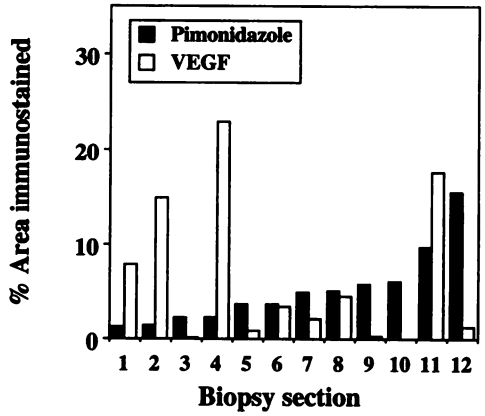

Fig. 3. Quantitative comparison between hypoxia and total VEGF expression (heavy immunostaining plus light immunostaining) in microscopic fields that both contained >1% of the area immunostained for pimonidazole adducts, and in which VEGF was also expressed. The data are derived from a quantitative image analysis of four to eight fields/section analyzed at ×200. No correlation between hypoxia and VEGF expression was observed.

VEGF expression. The half-maximal inhibition of 2-nitroimidazole binding by oxygen (0.4% gas-phase concentration; Ref. 15) is lower than that for VEGF up-regulation (0.8–2.2% gas-phase concentration; Ref. 5) in mammalian cells. Under these circumstances, pimonidazole binding will not identify all cells that are capable of inducing VEGF by a hypoxic mechanism. For example, cells immunostained for VEGF in close proximity to pimonidazole-stained cells (Fig. 1) might very well be at intermediate oxygen concentrations. However, oxygen gradients are continuous functions of the distances from blood vessels in experimental tumors (18), and this is presumably true for human tumors as well (19). Hypoxia marker data agree with this, in that tumor cells >10–12 cell diameters distant from blood vessels are consistently labeled with the marker in human and canine tumors with a wide variety of histologies (13, 16). Under these circumstances, the number of cells at intermediate oxygen concentrations is proportional to the number of hypoxic cells, so that a correlation between pimonidazole binding and VEGF expression, if it existed, should not be masked by VEGF arising in cells at intermediate oxygen levels. Perhaps of greater importance is the fact that VEGF is regulated by factors besides hypoxia, including the role that host cells play in producing VEGF (20). This could mask quantitative correlations between hypoxia and VEGF and, in particular, might account for the extensive immunostaining for VEGF in tumors that, according to the pimonidazole binding criterion, are well oxygenated (Fig. 2). The rate of VEGF production and loss in the tumors is unknown, but it is assumed that a steady state is maintained during the 24 h of the experiment, and that the lack of correlation between hypoxia and VEGF is not due to large shifts in steady-state VEGF concentrations from the time the hypoxic cells are labeled with pimonidazole to the time the tissue is harvested for analysis. Whereas the nutritional status of the hypoxic tumor cells identified in the present study is unknown, it is known that the reductive activation of pimonidazole requires NADH and/or NADPH. It seems unlikely, therefore, that the cells are nutritionally deprived to the extent that VEGF protein expression is inhibited, although this possibility cannot be ruled out completely.

A final consideration is that the immunohistochemical analysis of VEGF gives the number of cells that possess VEGF but not the concentration of VEGF within those cells. Nevertheless, it is VEGF measured by immunohistochemical assay that is correlated with microvascular density (6, 7) and that is of most interest to the present study. Contrary to a previous proposal (4), we conclude that the link between hypoxia and malignant progression cannot be established by merely measuring hypoxia and VEGF expression in squamous cell carcinomas at the time of clinical presentation. The results of the present study do not rule out the possibility that hypoxia promotes malignant progression through events occurring earlier in the natural history of human tumors.

References

1. Senger, D. R., Brown, L. F., Claffey, K. P., and Dvorak, H. F. Vascular permeability factor, tumor angiogenesis and stroma generation. Invasion Metastasis, *14:* 385–394, 1994.
2. Forsythe, J. A., Jiang, B. H., Iyer, N. V., Agani, F., Leung, S. W., Koos, R. D., and Semenza, G. L. Activation of vascular endothelial growth factor gene transcription by hypoxia-inducible factor 1. Mol. Cell. Biol., *16:* 4604–4613, 1996.
3. Damert, A., Ikeda, E., and Risau, W. Activator protein 1 binding potentiates the hypoxia-inducible factor 1-mediated, hypoxia-induced transcriptional activation of vascular endothelial growth factor expression in C6 glioma cells. Biochem. J., *327:* 419–423, 1997.
4. Shweiki, D., Itin, A., Soffer, D., and Keshet, E. Vascular endothelial growth factor induced by hypoxia may mediate hypoxia-initiated angiogenesis. Nature (Lond.), *359:* 843–845, 1992.
5. Leith, J. T., and Michelson, S. Secretion rates and levels of vascular endothelial growth factor in clone A or HCT-8 human colon tumour cells as a function of oxygen concentration. Cell Prolif., *28:* 415–430, 1995.
6. Takahashi, Y., Kitadai, Y., Bucana, C. D., Cleary, K. R., and Ellis, L. M. Expression of vascular endothelial growth factor and its receptor, KDR, correlates with vascularity, metastasis, and proliferation of human colon cancer. Cancer Res., *55:* 3964–3968, 1995.
7. Obermair, A., Kohlberger, P., Bancher, T. D., Tempfer, C., Sliutz, G., Leodolter, S., Reinthaller, A., Kainz, C., Breitenecker, G., and Gitsch, G. Influence of microvessel density and vascular permeability factor/vascular endothelial growth factor expression on prognosis in vulvar cancer. Gynecol. Oncol., *63:* 204–209, 1996.
8. Weidner, N. Intratumor microvessel density as a prognostic factor in cancer. Am. J. Pathol., *147:* 9–19, 1995.
9. Hockel, M., Schlenger, K., Aral, B., Mitze, M., Schaffer, U., and Vaupel, P. Association between tumor hypoxia and malignant progression in advanced cancer of the uterine cervix. Cancer Res., *56:* 4509–4515, 1996.
10. Raleigh, J. A., Miller, G. G., Franko, A. J., Koch, C. J., Fuciarelli, A. F., and Kelly, D. A. Fluorescence immunohistochemical detection of hypoxic cells in spheroids and tumours. Br. J. Cancer, *56:* 395–400, 1987.
11. Arteel, G. E., Thurman, R. G., Yates, J. M., and Raleigh, J. A. Evidence that hypoxia markers detect oxygen gradients in liver: pimonidazole and retrograde perfusion of rat liver. Br. J. Cancer, *72:* 889–895, 1995.
12. Azuma, C., Raleigh, J. A., and Thrall, D. E. Lifetime of hypoxic cells in spontaneous canine tumors. Radiat. Res., *148:* 35–42, 1996.
13. Kennedy, A. S., Raleigh, J. A., Perez, G. M., Calkins, D. P., Thrall, D. E., Novotny, D. B., and Varia, M. A. Proliferation and hypoxia in human squamous cell carcinoma of the cervix: first report of combined immunohistochemical assays. Int. J. Radiat. Oncol. Biol. Phys., *37:* 897–905, 1996.
14. Chapman, J. D., Franko, A. J., and Sharplin, J. A marker for hypoxic cells in tumours with potential clinical applicability. Br. J. Cancer, *43:* 546–550, 1981.
15. Gross, M. W., Karbach, U., Groebe, K., Franko, A. J., and Mueller-Klieser, W. Calibration of misonidazole labeling by simultaneous measurement of oxygen tension and labeling density in multicellular spheroids. Int. J. Cancer, *61:* 567–573, 1995.
16. Cline, J. M., Rosner, G. L., Raleigh, J. A., and Thrall, D. E. Quantification of CCI-103F labeling heterogeneity in canine solid tumors. Int. J. Radiat. Oncol. Biol. Phys., *37:* 655–662, 1997.
17. Raleigh, J. A., and Koch, C. J. Importance of thiols in the reductive binding of 2-nitroimidazoles to macromolecules. Biochem. Pharmacol., *40:* 2457–2464, 1990.
18. Helmlinger, G., Yuan, F., Dellian, M., and Jain, R. Interstitial pH and pO_2 gradients in solid tumors *in vivo*: high-resolution measurements reveal a lack of correlation. Nat. Med., *3:* 177–182, 1997.
19. Thomlinson, R. H., and Gray, L. H. The histological structure of some human lung cancers and the possible implications for radiotherapy. Br. J. Cancer, *9:* 539–549, 1955.
20. Claffey, K. P., and Robinson, G. S. Regulation of VEGF/VPF expression in tumor cells: consequences for tumor growth and metastasis. Cancer Metastasis Rev., *15:* 165–176, 1996.